General Disclaimer

One or more of the Following Statements may affect this Document

- This document has been reproduced from the best copy furnished by the organizational source. It is being released in the interest of making available as much information as possible.

- This document may contain data, which exceeds the sheet parameters. It was furnished in this condition by the organizational source and is the best copy available.

- This document may contain tone-on-tone or color graphs, charts and/or pictures, which have been reproduced in black and white.

- This document is paginated as submitted by the original source.

- Portions of this document are not fully legible due to the historical nature of some of the material. However, it is the best reproduction available from the original submission.

NASA

Technical Memorandum 84005

Postseismic Deformation Due to Subcrustal Viscoelastic Relaxation Following Dip-Slip Earthquakes

Steven C. Cohen

SEPTEMBER 1982

National Aeronautics and
Space Administration

Goddard Space Flight Center
Greenbelt, Maryland 20771

TM 84005

POSTSEISMIC DEFORMATION DUE TO SUBCRUSTAL VISCOELASTIC RELAXATION FOLLOWING DIP-SLIP EARTHQUAKES

by

Steven C. Cohen
Geodynamics Branch
Goddard Space Flight Center
Greenbelt, Maryland 20771

September 1982

GODDARD SPACE FLIGHT CENTER
Greenbelt, Maryland 20771

POSTSEISMIC DEFORMATION DUE TO SUBCRUSTAL VISCOELASTIC RELAXATION FOLLOWING DIP-SLIP EARTHQUAKES

Steven C. Cohen

ABSTRACT

The deformation of the earth following a dip-slip earthquake is calculated using a three-layer rheological model and finite element techniques. The three layers are an elastic upper lithosphere, a standard linear solid lower lithosphere, and a Maxwell viscoelastic asthenosphere-a model previously analyzed in the strike-slip case (Cohen, 1981, 1982). Attention is focused on the magnitude of the postseismic subsidence and the width of the subsidence zone that can develop due to the viscoelastic response to coseismic reverse slip. Detailed analysis for a fault extending from the surface to 15 km with a 45° dip reveals that postseismic subsidence is sensitive to the depth to the asthenosphere but is only weakly dependent on lower lithosphere depth. The greatest subsidence occurs when the elastic lithosphere is about 30 km thick and the asthenosphere lies just below this layer (asthenosphere depth = 2 times the fault depth). The extremum in the subsidence pattern occurs at about 5 km from the surface trace of the fault and lies over the slip plane. In a typical case after a time $t = 30\tau$ (τ = Maxwell time) following the earthquake the subsidence at this point is 60% of the coseismic uplift. Unlike the horizontal deformation following a strike-slip earthquake, significant vertical deformation due to asthenosphere flow persists for many times τ and the magnitude of the vertical deformation is not necessarily enhanced by having a partially relaxing lower lithosphere. The width of the postseismic subsidence zone also depends strongly on the depth to the asthenosphere and shows little sensitivity to the presence of a slowly relaxing lower lithosphere. The model fits postseismic rebound data from the 1896 Riku-u, Japan earthquake, but the fit is not substantially better than that obtained with a simpler two layer model. Previous estimates of the values of

asthenosphere depth (~30–40 km) and viscosity (~10^{20} poise) are confined by the three layer calculations.

POSTSEISMIC DEFORMATION DUE TO SUBCRUSTAL VISCOELASTIC RELAXATION FOLLOWING DIP-SLIP EARTHQUAKES

INTRODUCTION

During the past few years many papers have been published on models of crustal deformation during the earthquake cycle (e.g. Fitch and Scholz, 1971; Bischke, 1974; Rundle and Jackson, 1977; Scholz and Kato, 1978; Savage and Prescott, 1978; Spence and Turcotte, 1979; Melosh and Fleitout, 1982). Among the mechanisms proposed to account for various attributes of the temporal-spatial deformation patterns observed after earthquakes are surface afterslip, aseismic slip at depth (Thatcher, 1974), viscoelastic flow of subsurface layers of the earth (Nur and Mavko, 1974; Lehner and Li, 1981; Matsu'ura, 1981; Cohen, 1981), and various other forms of surface and subsurface yielding (Wahr and Wyss, 1980; Yang and Toksöz, 1981; Mavko, 1981). Comparisons of model calculations with geodetic measurements have revealed substantial agreement in a number of cases (e.g. Thatcher and Rundle, 1979; Brown et. al., 1977). Nevertheless, numerous questions remain unresolved about the most appropriate models to be used to represent the postseismic response to specific earthquakes. Many geodetic observations can be explained equally well by competing models and the qualitative and quantitative features of individual models sometimes show substantial variation depending on the choice of poorly constrained model parameters. Despite these problems progress has been made in putting numerical bounds on key descriptive parameters such as slip magnitude and depth, viscoelastic layer depths, and viscosity by performing detailed calculations with several models. With this in mind I have studied several layered viscoelastic models wherein layers of varying rheological constitutive laws and varying viscosity are distributed by depth (Cohen 1980, 1981, 1982). For example in this note and two previous papers an elastic upper lithosphere lies over a partially viscoelastic lower lithosphere, which in turn lies over an even more fluid asthenosphere. This is similar but not identical to the situation where an elastic lithosphere lies over a layered viscoelastic asthenosphere. A somewhat

different layering can occur if the lithosphere itself can be divided into an elastic upper crust, a decoupling intracrustal low viscosity zone, and an elastic lower lithosphere (Turcotte et. al. 1981). The purpose of the present paper is to complete my analysis of multilayer viscoelastic models by extending earlier calculations of postseismic rebound from strike-slip earthquakes to the case of dip-slip events.

MODEL DESCRIPTION AND RESULTS

The model I wish to consider divides the earth into three layers. All the layers are elastic in their bulk behavior. The top layer (upper lithosphere) is elastic in shear. Lying within this layer is a dislocation plane (fault) that dips at an angle θ from the horizontal and extends from an upper depth, d, to a lower depth, D. The layer thickness is H_1 and $0 \leq d \leq D \leq H_1$. The second layer (lower lithosphere) begins at depth H_1 and extends to depth H_2; its thickness is $H_2 - H_1$. This layer behaves as a standard linear solid in shear. The third layer (asthenosphere) begins at depth H_2. The layer acts as a Maxwell substance in shear. The rationale for this model is discussed in Cohen (1982). For the calculations reported here, the elastic moduli of the various layers are equal; the shear modulus has a value 3×10^{11} dyne/cm^2 and the bulk modulus the value 8.33×10^{11} dyne/cm^2. Viscosities of $\eta_a = 5 \times 10^{19}$ poise and $\eta_l = 1 \times 10^{21}$ poise are assumed for the asthenosphere and lower lithosphere respectively (Cohen, 1982). The asthenosphere extends to a depth of 300 km. The other parameters that enter the model are the fault depths d and D, layer depths, H_1 and H_2, and dip angle θ. The results depend on the coseismic fault slip, the time elapsed since the earthquake, and the location. The general differential equations for the displacements have already been published (Cohen, 1982); here we present results using a plane strain calculation. The plane is a cross section through the earth; the fault is a dipping line segment in this plane. Slip is paraliel to and along this line segment. The differential equations are solved by finite element techniques.

In Figure 1 I show an example of the vertical and horizontal displacements as a function of distance from the surface trace of the fault and of time after the earthquake. Qualitatively many of the features are similar to those observed in elastic lithosphere-viscoelastic asthenosphere (2-layer) calculations. The dominant feature of the vertical displacement pattern is the broad

postseismic subsidence over the fault and uplift further away. This general shape for the vertical displacements is maintained over a wide range of layer depths and dip angles when the fault is short enough that it does not rupture nearly all the lithosphere (Melosh, 1982). It is convenient for presenting figures to normalize the results to the coseismic slip, s_o and to take the unit of length as the fault depth, D (where for the results I will show, in Figures 3 and 4, d = 0). The unit of time is the Maxwell time of the asthenosphere $\tau = \eta_a/\mu_a$ where η_a and μ_a are the viscosity and rigidity respectively. Figure 2 shows an example of how the magnitude of the subsidence, ΔV_m, and the width of the subsidence zone, W, vary with time. As expected, ΔV_m changes most rapidly immediately after the earthquake when the asthenosphere begins to relax the high coseismic stress change. As stress relaxation proceeds, the subsidence rate decreases. The width of the subsidence zone generally grows at a decreasing rate with time. However, for a short time after the earthquake, the subsidence zone width decreases slightly before the longer term growth becomes dominant. The width of the subsidence zone is much broader than the coseismic uplift zone and in fact is larger than the depth to the asthenosphere, $W > H_2 \geq H_1 \geq D$. It is interesting to focus attention on how the subsidence varies with layer depths. Figure 3 shows the value of the postseismic vertical displacement, ΔV, ($t = 30\tau$) as a function of the lower lithosphere and asthenosphere depths. The distance chosen, $X = -1/3$ D, is near the extremum in the subsidence pattern. The interesting feature of Figure 3 is that ΔV fails to behave monotonically for either an increase in H_2 or H_1 with the other held fixed. For H_2 fixed, ΔV increases as H_1 increases until $H_1 > 2D$ then ΔV decreases. Similarly for H_1 fixed ΔV increases with H_2 until $H_2 > 2D$ then it decreases. Stated in another way: when the upper lithosphere thickness is more than 2D, subsidence is greatest when the lower lithosphere is vanishingly thin, when the upper lithosphere thickness is greater than 2D, subsidence is maximized when the lower lithosphere thickness, $T = 2D - H_1$. Similarly when the depth to the asthenosphere is less than 2D, subsidence is greatest when the lower lithosphere vanishes, but when the asthenosphere depth is greater than 2D, subsidence is maximum for $T = H_2 - 2D$. The greatest subsidence occurs when $H_1 = H_2 = 2D$. The condition for maximum subsidence $H_2 = 2D$ has been verified at other dip angles. The magnitude, $\Delta V = 0.26$, is approximately 60% of

the coseismic uplift in the present case. Another interesting feature of Figure 3 is that ΔV changes by only modest amounts over a substantial range of H_1 values. For example, when $H_1 = H_2 = 10/3$ D, $\Delta V = 0.19$, a value not that much less than the extremum value $\Delta V = 0.26$ at $H_1 = H_2 = 2D$. Only when H_2 gets small and the postseismic patterns change from those for which subsidence is dominant to those having substantial uplift do rapid changes in ΔV arise. For comparison with simpler two-layer models one can contrast the ΔV at various values of H_1 with those where $H_1 = H_2$ (i.e. viscoelastic lower lithosphere is vanishing thin).

In Figure 4 I plot the width of the subsidence zone, W, as a function of H_1 and H_2 (again at $X = -1/3$ D and $t = 30\tau$). The most striking feature is the growth of W with increasing H_2 and the relative insensitivity to H_1. The width of the deformation zone is dominated by the depth to the fastest relaxing layer, the fact that a shallower zone is also relaxing (at a slower rate) has little impact on the spatial pattern. In the case of postseismic rebound to slip on a strike-slip fault, the deformation due to asthenosphere flow is largely completed in a few Maxwell times. In the dip-slip case, however, it seems that the development of the deformation due to asthenosphere flow persists for much longer times. As a result, the existence of a relaxing viscoelastic rather than an elastic lower lithosphere does not necessarily enhance the long term subsidence.

Figure 5 compares the temporal and spatial patterns of the vertical displacement as changes are made in the fault depth. Curves 1 and 2 refer to faults that rupture the surface but extend to different depths; in this case the postseismic displacements are very comparable. By contrast, curve 3 refers to a fault that is buried and has the same length as that of curve 2 and the same lower depth as that of curve 1. The postseismic subsidence is much less in the buried fault case. Nevertheless, the shape of the postseismic deformation curves are similar in the three cases; certainly they are more similar than the coseismic curves.

For a comparison of model predictions to observations I have chosen the 1896 Riku-u, Japan earthquake. As discussed in Thatcher, et. al. (1980) the subsidence data for this region is derived from surveys in 1900, 1934, and 1974. The model results, shown in Figure 6 are derived for the

case where both the lithosphere and asthenosphere have thicknesses of 20 km. They confirm Thatcher's et.al. estimate of ~30 km for the lithosphere thickness and $\sim 10^{20}$ poise for the viscosity in this region of Japan. Despite the long time span of the record, little information is derived about the lower lithosphere viscosity. Its thickness however, must not be substantially greater than 20 km.

SUMMARY

In the postseismic rebound to strike-slip earthquakes the effect of having a lower lithosphere which is viscoelastic rather than elastic is to increase both the horizontal displacement magnitude and the time duration of the deformation process. The present study has shown that the vertical displacements after dip-slip earthquakes have a more complicated dependence on the existence of a relaxing lower lithosphere. However, over a wide range of layer depths the surface displacements are far less influenced by lower lithosphere relaxation than by asthenosphere relaxation. Because the magnitude, duration, and width of the postseismic subsidence depend primarily on the depth and viscosity of the most fluid layer geodetic data can be used to deduce asthenosphere depth and viscosity, but little information is obtained about the lower lithosphere.

REFERENCES

Bischke, R.E., "A model of convergent plate boundaries based on the recent tectonics of Shikoku, Japan," *J. Geophys. Res.*, 79, 4845-4857, 1974.

Brown, L.D., R.E. Reilinger, S.R. Holdahl, and E.I. Balazs, "Postseismic crustal uplift near Anchorage, Alaska," *J. Geophys. Res.*, 82, 3369-3378, 1977

Cohen, S.C., "Postseismic viscoelastic surface deformation and stress, 1. theoretical considerations, displacement and strain calculations," *J. Geophys. Res.*, 85, 3131-3150, 1980.

Cohen, S.C., "Postseismic rebound due to creep of the lower lithosphere and asthenosphere," *Geophys. Res. Lett.*, 8, 493-496, 1981.

Cohen, S.C., "A multilayer model of time dependent deformation following an earthquake on a strike-slip fault," *J. Geophys. Res.*, 87, 5409-5421, 1982.

Fitch, T.J., and C.H. Scholz, "Mechanisms of underthrusting in southwest Japan: a model of convergent plate interactions," *J. Geophys. Res.*, 76, 7260-7292, 1971.

Lehner, F.K., and V.C. Li, "Large-scale characteristics of plate boundary deformation related to the postseismic readjustment of a thin asthenosphere," Brown University Report No. 23, Providence, R.I., September, 1981.

Matsu'ura, M., T. Tanimoto, and T. Iwasaki, "Quasi-static displacements due to faulting in a layered half-space with an intervenient viscoelastic layer," *J. Phys. Earth*, 29 23-54, 1981.

Mavko, G.M., "Mechanics of motion on major faults," *Ann. Rev. Earth Planet. Sci.*, 9, 81-111, 1981.

Melosh, H.J., "Vertical movements following a dip-slip earthquake," SUNY report, Stony Brook, N.Y., January, 1982.

Melosh, H.J., and L. Feitout, "The earthquake cycle in subduction zone," *Geophys. Res. Lett.*, 9, 21-24, 1982.

Nur, A., and G. Mavko, "Postseismic viscoelastic rebound," *Science*, 183, 204-206, 1974.

Rundle, J.B., and D.D. Jackson, "A three-dimensional model of a strike-slip fault," *Geophys. J. R. Astro. Soc.*, 49, 575-591, 1977.

Savage J.C., and W.H. Prescott, "Asthenosphere readjustment and the earthquake cycle," *J. Geophys. Res.*, 83, 3369-3376, 1978.

Scholz, C.H., and T. Kato, "The behavior of a convergent plate boundary: crustal deformation in the South Kanto district, Japan," *J. Geophys. Res.*, 83, 783-797, 1978.

Spence, D.A., and D.L. Turcotte, "Viscoelastic Relaxation of Cyclic Displacements on the San Andreas Fault," *Proc. Roy. Soc., Ser A.*, 365, 121-144, 1979.

Thatcher, W., "Strain release mechanism of the 1906 San Francisco earthquake," *Science*, 184, 1283-1285, 1974.

Thatcher, W., and J.B. Rundle, "A model for the earthquake cycle in underthrust zones," *J. Geophys. Res.*, 84, 5540-5556, 1979.

Thatcher, W., T. Matsuda, T. Kato, and J.B. Rundle. "Lithosphere loading by the 1896 Riku-u earthquake, northern Japan: implications for plate flexure and asthenosphere rheology," *J. Geophys. Res.*, 85, 6429–6435, 1980.

Turcotte, D.L., J.Y. Liu, and F.H. Kulhawy, "Influences of rheology on the strain accumulation on the San Andreas fault," (abstract) *EOS, Trans. AGU*, 62, 1024, 1981.

Wahr, J. and M. Wyss, "Interpretation of postseismic deformation with a viscoelastic relaxation model," *J. Geophys. Res.*, 85, 6471–6477, 1980.

Yang, M. and M.N. Toksöz, "Time-dependent deformation and stress after a strike-slip earthquake," *J. Geophys. Res.*, 86, 2889–2901, 1981.

FIGURE CAPTIONS

Figure 1: Vertical displacements, V, and horizontal displacements, U, versus distance from fault at various times: coseismic displacements V_0, U_0 at time $t_0 = 0^+$; postseismic displacements $\Delta V = V(t_i) - V_0(t_0)$, $\Delta U = U(t_i) - U_0(t_0)$ at $t_i = 1 \cdot 10^9$ sec $= 6\tau$, $t_2 = 5 \cdot 10^9$ sec $= 30\tau$. Coseismic reverse slip = 1m, dip angle = 45°; fault depth = 0–15 km asthenosphere viscosity = $5 \cdot 10^{19}$ poise; lower lithosphere viscosity $1 \cdot 10^{21}$ poise.

Figure 2: Dependence of a subsidence extremum value, ΔV_m, and subsidence zone width W on time, t, for a model with $H_1/D = 4/3$; $H_2/D = 8/3$. Greatest subsidence occurs at $X = -1/3$ D. S_0 is coseismic dip and τ is Maxwell time of asthenosphere. Fault dip angle = 45°.

Figure 3: Magnitude of postseismic subsidence, ΔV, as a function of the depth of the asthenosphere, H_2, and lower lithosphere, H_1. Distance from fault, $X = -1/3$ D, time after earthquake, $t = 30\tau$. Other parameters are $\theta = 45°$, $\eta_1/\eta_a = 20$.

Figure 4: Width of postseismic subsidence zone, W, as a function of the depth of the asthenosphere, H_2, and lower lithosphere, H_1. Time after earthquake, $t = 30\tau$. Other parameters are $\theta = 45°$, $\eta_1/\eta_a = 20$.

Figure 5: Vertical displacements for various fault depths: curve 1: d = 0 km, D = 15 km; curve 2: d = 0 km, D = 10 km; curve 3: d = 5 km, D = 15 km.

Figure 6: Comparison of leveling data and model calculations for postseismic rebound to 1896 Riku-u Japan earthquake a. 1934–1900 data; b. 1974–1900 data. Survey results use a 3-point smoothing to data of Thatcher, et. al (1980). Model parameters are coseismic slip = 2 m, fault depth = 0–15 km; dip angle = 45°; asthenosphere depth = 40 km; asthenosphere viscosity = 5×10^{19} poise, lower lithosphere depth = 20 km, lower lithosphere viscosity = 1×10^{21} poise.

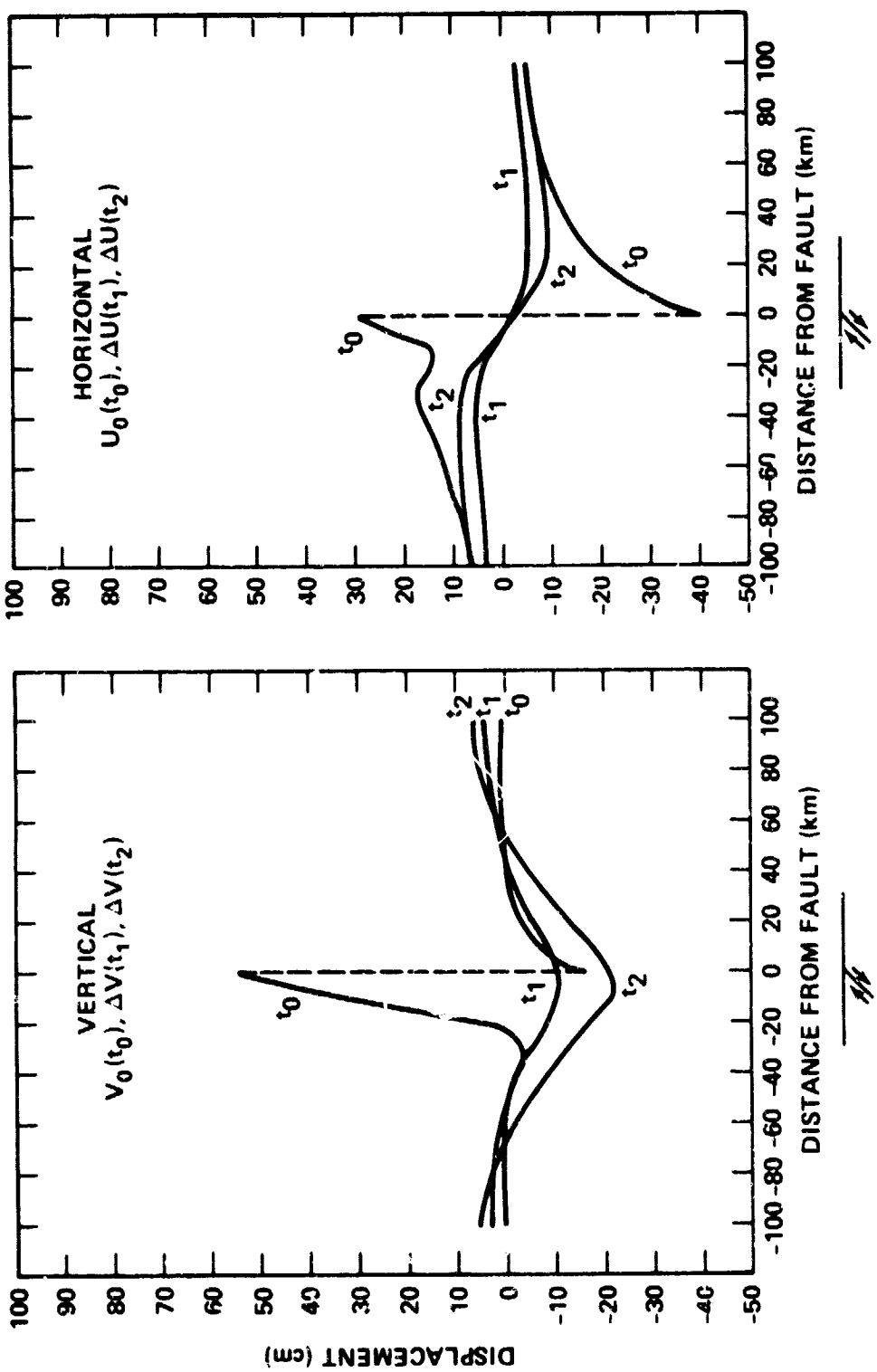

Figure 1. Vertical displacements, V, and horizontal displacements, U, versus distance from fault at various times: coseismic displacements V_0, U_0 at time $t_0 = \infty$; postseismic displacements $\Delta V = V(t_i) - V_0(t_0)$, $\Delta U = U(t_i) - U_0(t_0)$ at $t_1 = 1 \cdot 10^9$ sec = 6 τ, $t_2 = 5 \cdot 10^9$ sec = 30 τ. Coseismic reverse slip = 1m, dip angle = 45°; fault depth = 0–15 km asthenosphere viscosity = $5 \cdot 10^{19}$ poise; lower lithosphere viscosity $1 \cdot 10^{21}$ poise.

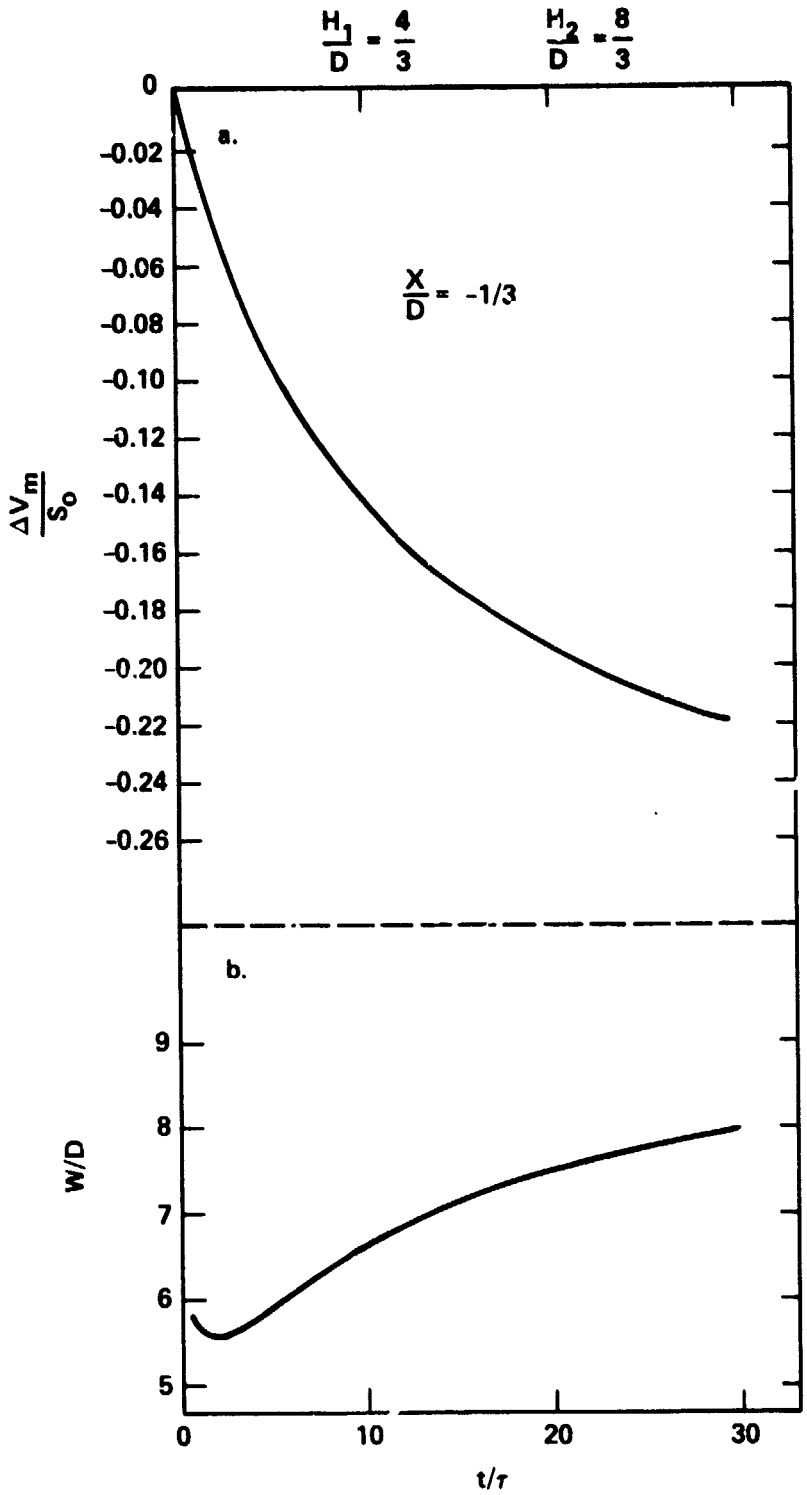

Figure 2. Dependence of a subsidence extremum value, ΔV_m, and subsidence zone width W on time, t, for a model with $H_1/D = 4/3$; $H_2/D = 8/3$. Greatest subsidence occurs at X = -1/3 D. S_o is coseismic dip and τ is Maxwell time of asthenosphere. Fault dip angle = 45°.

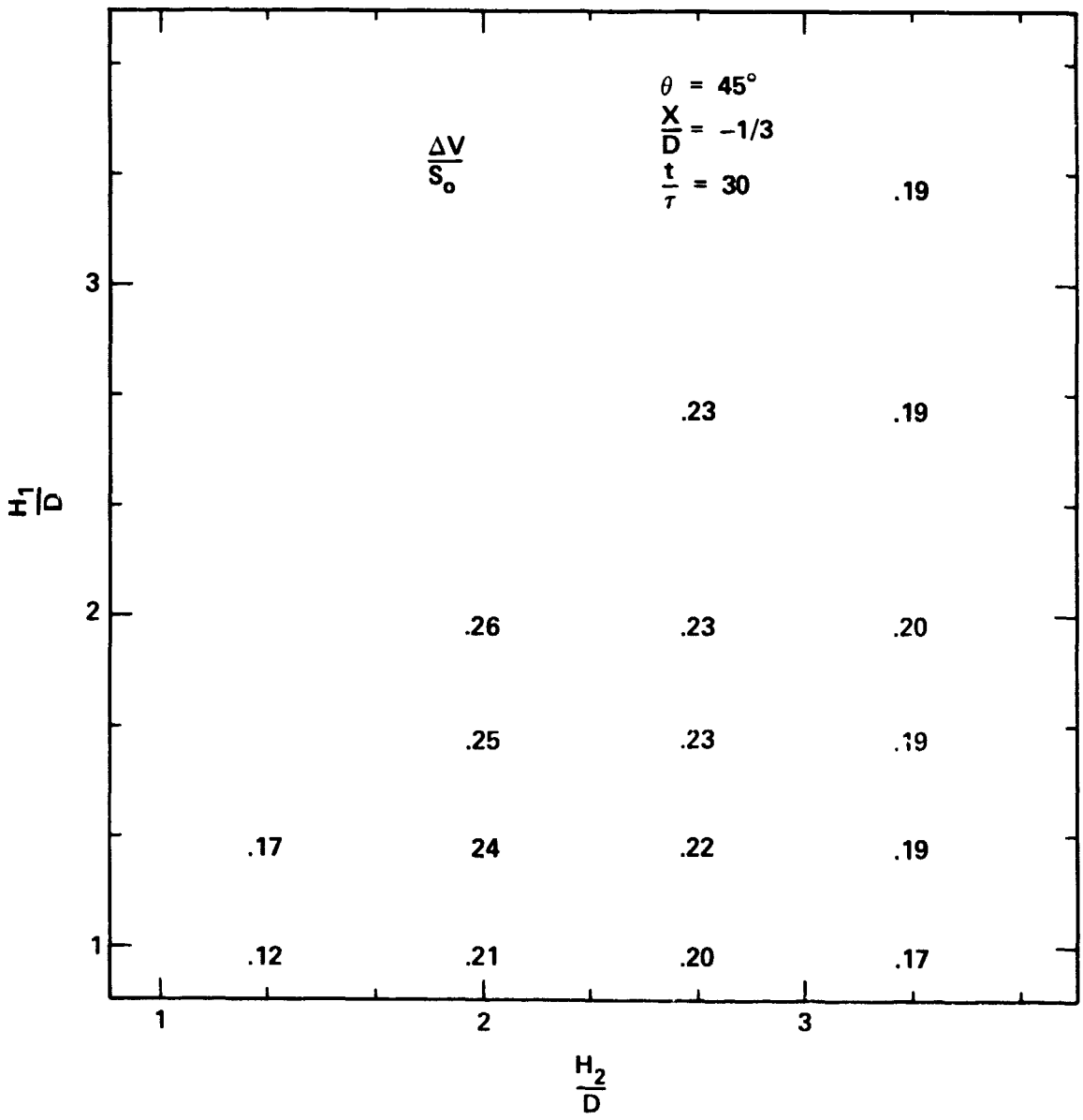

Figure 3. Magnitude of postseismic subsidence, ΔV, as a function of the depth of the asthenosphere, H_2, and lower lithosphere, H_1. Distance from fault, X = -1/3 D, time after earthquake, t = 30 τ. Other parameters are $\theta = 45°$, $\eta_l/\eta_a = 20$.

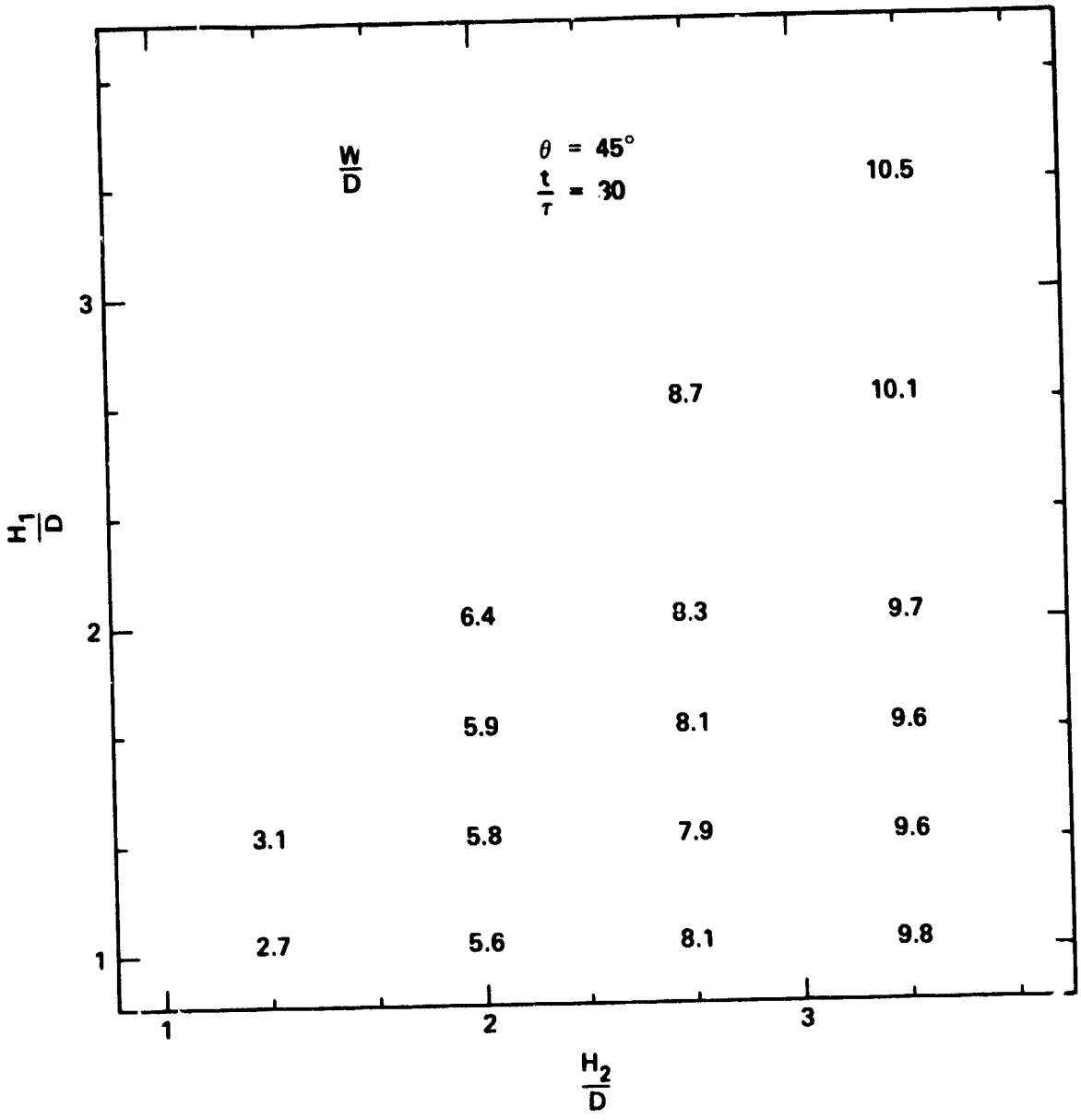

Figure 4. Width of postseismic subsidence zone, W, as a function of the depth of the asthenosphere, H_2, and lower lithosphere, H_1. Time after earthquake, t = 30 τ. Other parameters are $\theta = 45°$, $\eta_1/\eta_a = 20$.

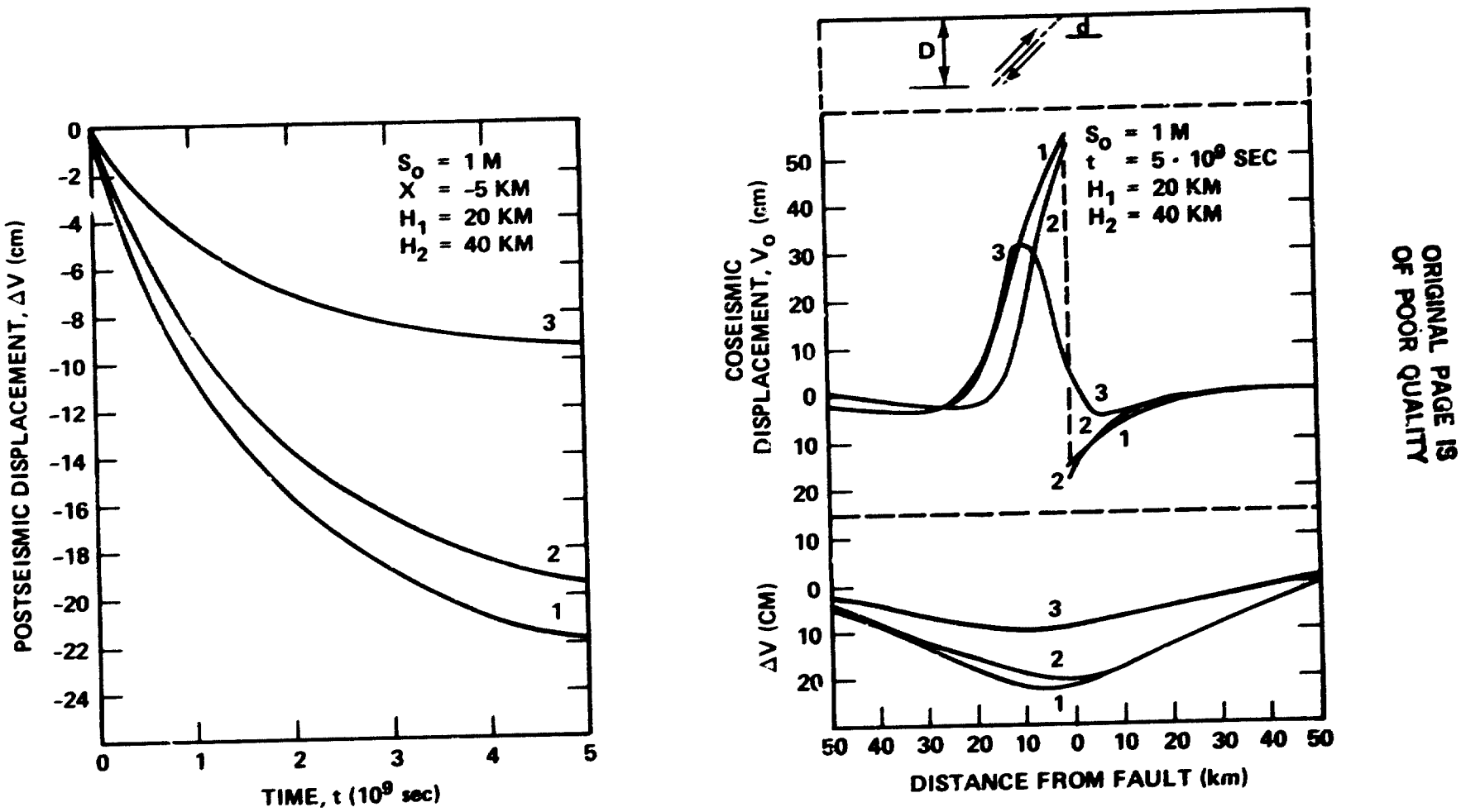

Figure 5. Vertical displacements for various fault depths: curve 1:d = 0 km, D = 15 km; curve 2:d = 0 km, D = 10 km; curve 3: d = 5 km, D = 15 km.

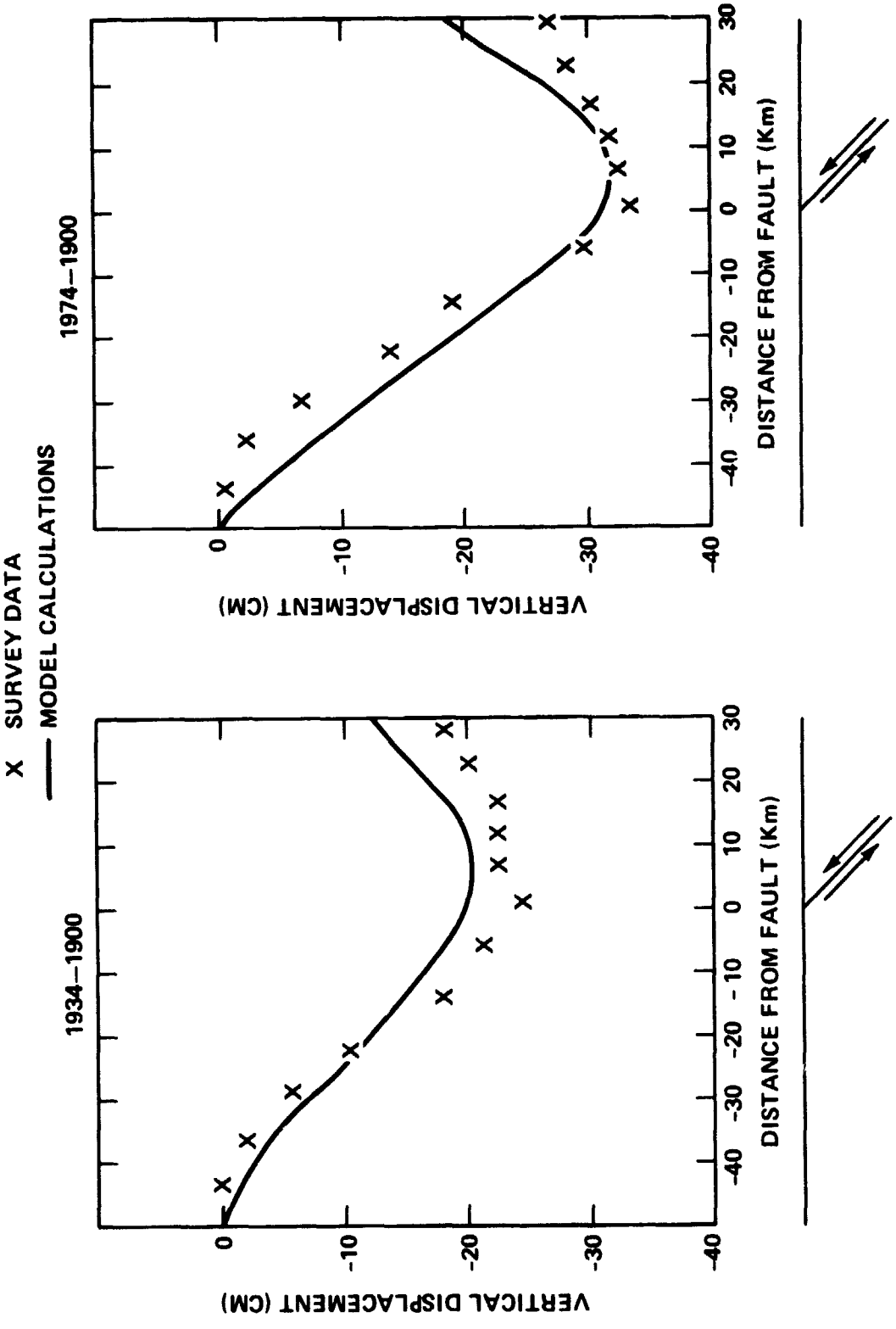

Figure 6. Comparison of leveling data and model calculations for postseismic rebound to 1896 Riku-u Japan earthquake a. 1934–1900 data; b. 1979–1900 data. Survey results use a 3-point smoothing to data of Thatcher, et.al. (1980). Model parameters are coseismic slip = 2 m, fault depth = 0–15 km; dip angle = 45°; asthenosphere depth = 40 km; asthenosphere viscosity = 5×10^{19} poise, lower lithosphere depht = 20 km, lower lithosphere viscosity = 1×10^{21} poise.